Mueller-Stokes characterization and optimization of a liquid crystal on silicon display showing depolarization

A. Márquez[1*], I. Moreno[2], C. Iemmi[3], A. Lizana[4], J. Campos[4], and M. J. Yzuel[4]

[1]*Dept. de Física, Ingeniería de Sistemas y Teoría de la Señal, Universidad de Alicante, Ap. 99, 03080 Alicante, Spain*
[2]*Dept. de Ciencia de Materiales, Óptica y Tecnología Electrónica, Universidad Miguel Hernández, Elche, Spain*
[3]*Dept. de Física, Fac. de Ciencias Exactas y Naturales, Universidad de Buenos Aires, 1428 Buenos Aires, Argentina*
[4]*Departamento de Física, Universidad Autónoma de Barcelona, 08193 Bellaterra, Spain*
**Corresponding author: andres.marquez@ua.es*

Abstract: In this paper we characterize the polarimetric properties of a liquid crystal on silicon display (LCoS), including depolarization and diattenuation which are usually not considered when applying the LCoS in diffractive or adaptive optics. On one hand, we have found that the LCoS generates a certain degree (that can be larger than a 10%) of depolarized light, which depends on the addressed gray level and on the incident state of polarization (SOP), and can not be ignored in the above mentioned applications. The main origin of the depolarized light is related with temporal fluctuations of the SOP of the light reflected by the LCoS. The Mueller matrix of the LCoS is measured as a function of the gray level, which enables for a numerical optimization of the intensity modulation configurations. In particular we look for maximum intensity contrast modulation or for constant intensity modulation. By means of a heuristic approach we show that, using elliptically polarized light, amplitude-mostly or phase-mostly modulation can be obtained at a wavelength of 633 nm.

OCIS codes: (120.2040) Displays; (120.5410) Polarimetry; (230.3720) Liquid-crystal devices; (230.6120) Spatial light modulators.

References and links

1. H.-K. Liu, J. A. Davis and R. A. Lilly, "Optical-data-processing properties of a liquid-crystal television spatial light modulator," Opt. Lett. **10**, 635-637 (1985).
2. H. J. Coufal, D. Psaltis and B. T. Sincerbox, eds., *Holographic Data Storage*, (Springer-Verlag, Berlin, 2000).
3. R. Dou and M. K. Giles, "Closed-loop adaptive optics system with a liquid crystal television as a phase retarder," Opt. Lett. **20**, 1583-1585 (1995).
4. A. Márquez, C. Iemmi, J. Campos, J. C. Escalera and M. J. Yzuel, "Programmable apodizer to compensate chromatic aberrations effects using a liquid crystal spatial light modulator," Opt. Express **13**, 716-730 (2005).
5. R. Tudela, E. Martín-Badosa, I. Labastida, S. Vallmitjana, I. Juvells and A. Carnicer, "Full complex Fresnel holograms displayed on liquid crystal devices," J. Opt. A: Pure Appl. Opt. **5**, S189-S194 (2003).
6. W. Osten, C. Kohler and J. Liesener, "Evaluation and application of spatial light modulators for optical metrology," Opt. Pura Apl. **38**, 71-81 (2005).
7. A. Márquez, C. Iemmi, I. Moreno, J. A. Davis, J. Campos and M. J. Yzuel, "Quantitative prediction of the modulation behavior of twisted nematic liquid crystal displays based on a simple physical model," Opt. Eng. **40**, 2558-2564 (2001).
8. J. Nicolás, J. Campos and M. J. Yzuel, "Phase and amplitude modulation of elliptic polarization states by nonabsorbing anisotropic elements: application to liquid-crystal devices," J. Opt. Soc. Am. A **19**, 1013-1020 (2002).
9. S. T. Wu and D. K. Yang, *Reflective Liquid Crystal Displays*, (John Wiley & Sons Inc., Chichester, 2005).
10. Y. Lee, J. Gourlay, W. J. Hossack, I. Underwood and A. J. Walton, "Multi-phase modulation for nematic liquid crystal on silicon backplane spatial light modulators using pulse-width modulation driving scheme," Opt. Commun. **236**, 313-322 (2004).

#86144 - $15.00 USD Received 8 Aug 2007; revised 18 Oct 2007; accepted 18 Oct 2007; published 24 Jan 2008

11. J. Gourlay, P. McOwan, D. G. Vass, I. Underwood and M. Worboys, "Time-multiplexed optical Hadamard image transforms with ferroelectric-liquid-crystal-over-silicon spatial light modulators," Opt. Lett. **18**, 1745-1747 (1993).
12. Q. Mu, Z. Cao, L. Hu, D. Li and L. Xuan, "Adaptive optics imaging system based on a high resolution liquid crystal on silicon device," Opt. Express **14**, 8013-8018 (2006).
13. H. Dai, K. Xu, Y. Liu, X. Wang and J. Liu, "Characteristics of LCoS Phase-only spatial light modulator and its applications," Opt. Commun. **238**, 269-276 (2004).
14. T. Ito, T. Shimobaba, H. Godo and M. Horiuchi, "Holographic reconstruction with a 10-μm pixel-pitch reflective liquid-crystal display by use of a light-emitting diode reference light," Opt. Lett. **27**, 1406-1408 (2002).
15. K. P. Proll, J. M. Nivet, K. Körner and H. J. Tiziani, "Microscopic three-dimensional topometry with ferroelectric liquid-crystal-on-silicon displays," Appl. Opt. **42**, 1773-1778 (2003).
16. J. Kacperski and M. Kujawinska, "Active, LCoS based laser interferometer for microelements studies," Opt. Express **14**, 9664-9678 (2006).
17. K. Lu and B. E. A. Saleh, "Theory and design of the liquid crystal TV as an optical spatial phase modulator," Opt. Eng. **29**, 240-246 (1990).
18. A. Márquez, J. Campos, M. J. Yzuel, I. Moreno, J. A. Davis, C. Iemmi, A. Moreno and A. Robert, "Characterization of edge effects in twisted nematic liquid crystal displays," Opt. Eng. **39**, 3301-3307 (2000).
19. Q. Wang and S. He, "A new effective model for the director distribution of a twisted nematic liquid crystal cell," J. Opt. A: Pure Appl. Opt. **7**, 438-444 (2005).
20. I. Moreno, P. Velásquez, C. R. Fernández-Pousa, M. M. Sánchez-López and F. Mateos, "Jones matrix method for predicting and optimizing the optical modulation properties of a liquid-crystal display," J. Appl. Phys. **94**, 3697-3702 (2003).
21. V. Durán, J. Lancis, E. Tajahuerce, and Z. Jaroszewicz, "Equivalent retarder-rotator approach to on-state twisted nematic liquid crystal displays," J. Appl. Phys. **99**, 113101-113106 (2006).
22. D. Goldstein, *Polarized Light* (Marcel Dekker, 2004).
23. J. L. Pezzanitti and R. A. Chipman, "Phase-only modulation of a twisted nematic liquid-crystal TV by use of the eigenpolarization states," Opt. Lett. **18**, 1567-1569 (1993).
24. J. A. Davis, I. Moreno and T. Tsai, "Polarization eigenstates for twisted-nematic liquid-crystal displays," Appl. Opt. **37**, 937-945 (1998).
25. J. L. Pezzaniti, S. C. McClain, R. A. Chipman and S.-Y. Lu, "Depolarization in liquid-crystal televisions," Opt. Lett. **18**, 2071-2073 (1993).
26. J. E. Wolfe and R. A. Chipman, "Polarimetric characterization of liquid-crystal-on-silicon panels," Appl.Opt. **45**, 1688-1703 (2006).
27. "IEC 61947-1:2002. Electronic Projection. Measurement and documentation of key performance criteria. Part 1: Fixed resolution projectors", IEC (International Electrotechnical Commission), Geneva, 2002.
28. J. Campos, I. Moreno, A. Márquez, C. Iemmi, V. Mariscal , J. A. Davis and M. J. Yzuel, "Simple Jones Method for describing Modulation Properties of Reflective Liquid Crystal Spatial Light Modulators," in *CP860. Information Optics: 5th International Workshop*, G. Cristóbal, B. Javidi and S. Vallmitjana, eds. (AIP, 2006), pp. 159-168.
29. S.-Y. Lu and R. A. Chipman, "Interpretation of Mueller matrices based on polar decomposition," J. Opt. Soc. Am. A **13**, 1106-1113 (1996).
30. S.-Y. Lu and R. A. Chipman, "Homogeneous and inhomogeneous Jones matrices," J. Opt. Soc. Am. A **11**, 766-773 (1994).
31. S. Stallinga, "Equivalent retarder approach to reflective liquid crystal displays," J. Appl. Phys. **86**, 4756-4766 (1999)
32. A. Márquez, I. Moreno, J. Campos and M. J. Yzuel, "Analysis of Fabry-Perot interference effects on the modulation properties of liquid crystal displays," Opt. Commun. **265**, 84-94 (2006).
33. A. Bergeron, J. Gauvin, F. Gagnon, D. Gingras, H. H. Arsenault and M. Doucet, "Phase calibration and applications of a liquid-crystal spatial light modulator," Appl. Opt. **34**, 5133-5139 (1995).
34. D. Engström, G. Milewski, J. Bengtsson and S. Galt, "Diffraction-based determination of the phase modulation for general spatial light modulators," Appl. Opt. **45**, 7195-7204 (2006).
35. I. Moreno, J. Campos, C. Gorecki and M. J. Yzuel, "Effects of amplitude and phase mismatching errors in the generation of a kinoform for pattern recognition," Jpn. J. Appl. Phys. **34**, 6423-6434 (1995).
36. I. Moreno, C. Iemmi, A.Márquez, J. Campos and M. J. Yzuel, "Modulation light efficiency of diffractive lenses displayed onto a restricted phase-mostly modulation display," Appl. Opt. **43**, 6278-6284 (2004).

1. Introduction

Liquid crystal displays (LCD) have found widespread use as spatial light modulators (SLM) in applications such as optical image processing [1], holographic data storage [2], programmable adaptive optics [3], diffractive optics [4,5] and optical metrology [6]. They can

#86144 - $15.00 USD Received 8 Aug 2007; revised 18 Oct 2007; accepted 18 Oct 2007; published 24 Jan 2008

be used as amplitude-only SLMs or as phase-only SLMs when properly selecting the input and output polarization configurations [7,8]. In recent years a new LCD technology, liquid crystal on silicon (LCoS) based displays, has attracted considerable interest due to some important manufacturing improvements leading in many aspects to a superior performance [9,10]. LCoS displays are based on silicon CMOS technology, which enables for a relatively inexpensive display showing a very high resolution with pixel sizes less than ten microns and with a fill factor exceeding the 90%. They are reflective displays which, due to the double pass through the device, enables for an increase in the dynamic modulation range, especially important in applications requiring phase-shift modulation of the incident wavefront. Simultaneously they have a small cell thickness (less than 1 μm is feasible), which enables for a rapid response. LCoS have already shown its ability to work as SLMs in optical image processing [11], programmable adaptive optics [12], diffractive optics [13], 3-D holographic display [14] and optical metrology [15,16].

In general, when using commercial LCDs the researcher does not have access to the value of a set of parameters defining the electrooptic modulation properties of the LC device. Researchers have proposed a series of reverse engineering models [17-21], usually based on the Jones matrix polarization formalism [22], to describe the modulation capabilities of LCDs. In general these models provide an approximate description of the profile of the electrooptic properties of the LC across the depth of the cell [17-19]. Other approaches concentrate on the numerical evaluation of the matrix elements of the Jones matrix describing the LCD [20], or consider the LCD as a lossless non-depolarizing polarization device, and regard it as a retarder – rotator combination [21]. Jones matrix models generally account both for the amplitude and phase-shift modulation capabilities of LCDs.

The Mueller matrix formalism provides an alternative polarimetric description of polarization phenomena, and it has been also applied to calibrate the response of LCDs. Pezzaniti and Chipman [23] measured the Mueller matrix of a LCD to calculate its average eigenpolarization states in order to obtain phase-only modulation. One of the two orthogonal average eigenpolarizations provides a high range of phase-shift [24] with a reasonably flat amplitude modulation. In another work Pezzaniti et al. [25] reported the existence of LCDs showing a certain degree of depolarized light. More recently Wolfe and Chipman [26] showed that a full polarimetric characterization of LCoS devices is a more complete and suitable approach than the standard radiometric characterization typically followed by the display industry in quality control tests [27]. In their study they found a certain degree of depolarized light and the inhomogeneity in various polarimetric parameters across the LCoS aperture.

The existence of depolarized light [22] may lead to the degradation in the application of the LCoS as a SLM. This effect can not be calibrated and evaluated with the models described in Refs. [17-21]. The ability for a device showing depolarization to be used in amplitude-only or in phase-only modulation regimes is a novel and necessary study. In principle, it can be expected that depolarized light may be added incoherently as a non-uniform background across the aperture of the LCoS because the degree of polarization may depend on factors such as the addressed gray level and the incident SOP.

In this paper we characterize the polarimetric properties of a liquid crystal on silicon display (LCoS), therefore including depolarization and diattenuation which are usually not considered when applying the LCoS in non-display applications. In this polarimetric study we include time measurements that show the phenomenon responsible for the depolarization. Along with the polarimetric characterization we measure the Mueller matrix of the LCoS as a function of the gray level. The Mueller matrix characterization enables for a numerical search of optimum intensity modulation configurations. In particular we look for maximum contrast modulation or constant intensity modulation. We demonstrate that in general the best results are obtained when using elliptically polarized light. By means of a heuristic approach we show that amplitude-mostly modulation or phase-mostly modulation with a large phase-shift modulation depth can also be obtained.

The paper is organized as follows. In Section 2 we measure the Stokes vector for a series of input SOPs. These measurements serve to analyse the depolarization and the diattenuation

#86144 - $15.00 USD Received 8 Aug 2007; revised 18 Oct 2007; accepted 18 Oct 2007; published 24 Jan 2008

produced by the device. In Section 2 we also analyse the origin for the depolarized light produced by the LCoS. In Section 3 we use the Stokes vectors measurements to calculate the Mueller matrix for the LCoS, and we proof the capability of the Mueller matrix to predict the SOP of the light reflected by the LCoS. In Section 4, by means of a numerical search and using the Mueller matrix for the LCoS we optimize the intensity transmission for specific modulation regimes. The main conclusions of the paper are given in Section 5.

2. Stokes parameters: analysis of the depolarization and the diattenuation in a LCoS

2.1 Experimental setup

In this work we use a Philips LCoS model X97c3A0, sold as the kit LC-R2500 by Holoeye. The LC-R2500 is a 2.46 cm diagonal monochrome reflective LCoS of the 45º twisted nematic type, with XGA resolution (1024 x 768 pixels), with digital data input and digitally controlled gray scales with 256 gray levels. The pixels are square with a pixel center to center separation of 19 μm and a fill factor of 93%. Preliminary results obtained with the LCoS show that a certain degree of depolarized light is produced [28]. To obtain a full polarimetric characterization of the LCoS we proceed with the measurement of the Stokes parameters for the SOP of the light reflected by the LCoS for a series of input SOPs. The input SOPs have been chosen so that the Mueller matrix of the device can also be calculated from these measurements (see Section 3 for the resulting Mueller matrix).

In the experimental setup we use the unexpanded laser beam from a He-Ne laser (λ=633 nm) at non-perpendicular incidence onto the LCoS, to separate the incident and the reflected beams of light. The angle of incidence with respect to the normal of the LCoS is 2º. We want almost-perpendicular illumination in order to decouple the polarizing effects of the LCoS from the polarizing effects introduced by the Fresnel coefficients with the angle of incidence. The use of a beam-splitter to ensure perpendicular illumination of the LCoS would have added additional polarizing effects.

A polarization state generator (PSG) and a polarization state detector (PSD), respectively before and behind the LCoS, composed of a linear polarizer and a quarter wavelength wave plate are needed for the polarimetric characterization [22]. We use linear polarizers model DMP-200-VIS1, and wave plates model AQM-100-545, corresponding to achromatic quarter wave plates in the visible, both by Meadowlark Optics. We verified that the retardance of the wave plates is 90º at 633 nm. With the PSG and the PSD we can generate and detect any possible SOP. For the polarimetric characterization we generate and detect 6 different SOPs: linearly polarized along the vertical, horizontal, at 45º and at -45º, and right-handed and left-handed circularly polarized light (labelled in the following as X, Y, 45, -45, R and L, respectively). In these experiments we measure the irradiance for the light after the PSD. For the measurements we use the radiometer model 1830-C, by Newport.

Next we introduce the sign convention used in this work, which is consistent with the convention followed for example by Goldstein [22]. To express the light incident and the light reflected by the LCoS we consider the corresponding right-handed reference systems for the incident and the reflected paths. In these systems the X axis is along the vertical of the lab, the Z axis points along the propagation of the light beam, and the Y axis is inverted after reflection. The origin for the angles for the polarization elements (linear polarizers and wave plates) is taken with respect to the vertical of the lab, and the sense is taken positive for a counter-clockwise rotation (the observer looking in the opposite sense of the propagation of the light beam). In the case of the azimuth ψ and the ellipticity χ angles describing a specific SOP a diagram is given in Fig. 1, where we show the reference systems for the lab (X and Y axes) and for the proper axes of the ellipse (X' and Y' axes, with X' the major axis). The azimuth angle ψ ($0 \le \psi < \pi$) accounts for the orientation of the major axis of the ellipse with respect to the X axis. Its sense is positive for a counter-clockwise rotation. The ellipticity angle χ ($-\pi/4 \le \chi \le \pi/4$) is taken from the major axis of the polarization ellipse to one of the diagonals of the rectangle circumscribing the ellipse. It is considered positive for right-handed SOPs, which corresponds to a rotation of the electric field in the clockwise sense. In Fig. 1

#86144 - $15.00 USD Received 8 Aug 2007; revised 18 Oct 2007; accepted 18 Oct 2007; published 24 Jan 2008

both the azimuth and the ellipticity angles are positive according to this sign convention. We note that in the representation in the Poincaré sphere we plot right-handed SOPs on the north hemisphere as in Ref. [22].

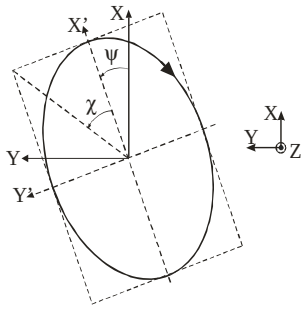

Fig. 1. Polarization ellipse. The azimuth ψ and the ellipticity χ angles indicated in the figure have a positive value according to the sign convention explained in the text.

Given a specific input SOP generated by the PSG, to obtain the 4 components (S_0, S_1, S_2 and S_3) of the Stokes vector for the SOP reflected by the LCoS we follow the standard procedure [22],

$$\begin{pmatrix} S_0 \\ S_1 \\ S_2 \\ S_3 \end{pmatrix} = \begin{pmatrix} I_0 \\ I_x - I_y \\ I_{45} - I_{-45} \\ I_R - I_L \end{pmatrix} \tag{1}$$

where I_x, I_y, I_{45}, I_{-45}, I_R and I_L are respectively the intensities measured at the exit of the PSD from the projection of the reflected SOP onto the 6 corresponding SOPs (X, Y, 45, -45, R and L) for which the PSD is configured. The value for these intensities is corrected from the attenuation due to the transmission through the PSD. The magnitude I_0 is the total intensity reflected by the LCoS. For normalization purposes, an additional measurement is taken, the intensity of the light incident onto the LCoS: each measurement is then divided by the incident intensity. Thus, variations in the laser output or in the PSD transmission do not have any effect in the final results.

The precision in the measurement of the Stokes parameters measured in this work can be roughly estimated as ±0.02. For this estimation we consider both an uncertainty of ±1º in the orientation of the polarizing elements in the setup, and an uncertainty of 1% in the intensity measured with the radiometer. From these two sources of error, the former, i.e. uncertainty in the orientation of the polarizing elements, has a negligible contribution.

2.2 Experimental results: Depolarization, diattenuation and retardance performance

From the Stokes measurements we can obtain both the degree of polarization (DoP) of the reflected light and the diattenuation coefficient of the LCoS. The DoP of the reflected light is calculated as [22],

$$DoP = \frac{\sqrt{S_1^2 + S_2^2 + S_3^2}}{S_0} \tag{2}$$

In Fig. 2 we show the DoP as a function of the gray level and for the six different input SOPs (X, Y, 45, -45, R and L). Note that the vertical scale ranges from 0.80 to 1.05. We see that the DoP varies both with the gray level and with the incident SOP. In particular the amount of depolarized light produced by the LCoS can reach values as large as 10%. This happens in the gray level range about 180-200 and for incident SOPs 45 and -45. In principle, this is a high value of depolarized light produced by the LCoS. To characterize a system with

#86144 - $15.00 USD Received 8 Aug 2007; revised 18 Oct 2007; accepted 18 Oct 2007; published 24 Jan 2008

depolarization the Mueller matrix formalism has to be used, as we do in Section 3. We note that the uncertainty in the calculated DoP, due to the ±0.02 uncertainty in the Stokes parameters, can be estimated as ±0.04 in the various DoP results presented along this work. This uncertainty may lead in some configurations and certain gray levels to values of DoP slightly over 1, situations where we can consider that the light is fully polarized.

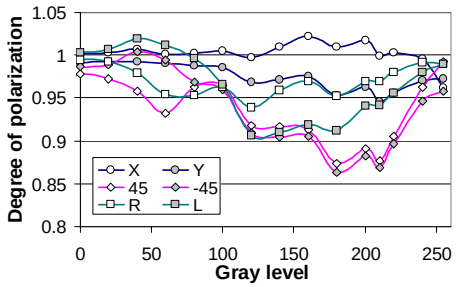

Fig. 2. Degree of polarization for the 6 input SOPs.

The diattenuation measures the difference in transmission between two incident orthogonal SOPs [22], thus, combining the 6 SOPs (X, Y, 45, -45, R and L) generated by the PSG the following three diattenuation components can be defined,

$$D_X = \frac{S_0^X - S_0^Y}{S_0^X + S_0^Y},\ D_{45} = \frac{S_0^{45} - S_0^{-45}}{S_0^{45} + S_0^{-45}},\ D_C = \frac{S_0^R - S_0^L}{S_0^R + S_0^L} \tag{3}$$

where S_0^X, S_0^Y, S_0^{45}, S_0^{-45}, S_0^R and S_0^L corresponds to the intensity reflected by the LCoS for the 6 different input SOPs generated by the PSG. The total diattenuation is given by,

$$D = \frac{S_0^{\max} - S_0^{\min}}{S_0^{\max} + S_0^{\min}} \tag{4}$$

It represents the difference in transmission between the two SOPs with the highest $S_0^{\max}$ and the lowest $S_0^{\min}$ intensity transmission respectively. These SOPs are orthogonal to each other. The total diattenuation can also be calculated from the components defined in Eq. (3) as,

$$D = \sqrt{D_X^2 + D_{45}^2 + D_C^2} \tag{5}$$

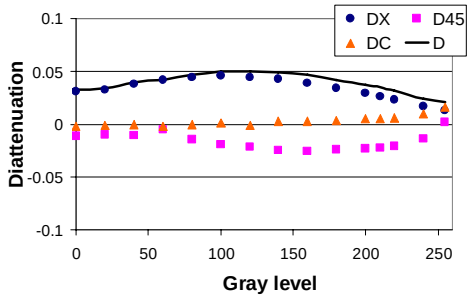

Fig. 3. Values for the three diattenuation components and for the total diattenuation.

#86144 - $15.00 USD Received 8 Aug 2007; revised 18 Oct 2007; accepted 18 Oct 2007; published 24 Jan 2008

Using Eqs. (3) and (5) we can calculate the value for the diattenuation parameters. In Fig. 3 we plot their values as a function of the gray level. We note that the vertical scale is zoomed between 0.1 and -0.1. We see that the maximum value for the total diattenuation is about 0.05. Therefore it can be said that the diattenuation is negligible and the LCoS can be basically considered as the combination of a retarder and a depolarizer as given in Ref. [29].

To analyze the action as a retarder we calculate the normalized Stokes components S_{n1}, S_{n2}, and S_{n3} as,

$$S_{n1,n2,n3} = \frac{S_{1,2,3}}{I_{pol}}, \tag{6}$$

where

$$I_{pol} = \sqrt{S_1^2 + S_2^2 + S_3^2} \tag{7}$$

is the intensity due to the polarized component of the reflected SOP [22]. The normalized Stokes vector $(1\ S_{n1}\ S_{n2}\ S_{n3})^{\perp}$ ($\perp$ means transpose) represents the component of fully polarized light, normalized to unit intensity, for the Stokes vector in Eq. (1). In Fig. 4 we plot the vector $(1\ S_{n1}\ S_{n2}\ S_{n3})^{\perp}$, as a function of the addressed gray level. For this purpose, two complementary representations are given, one using the Poincaré sphere [Figs. 4(a), 4(c), and 4(e)] and one plotting the azimuth and ellipticity of the SOP as a function of the gray level [Figs. 4(b), 4(d), and 4(f)]. The trajectory along the Poincaré sphere provides a fast visualization for the range of reflected SOPs, and the azimuth and ellipticity plot as function of the gray level provides a more quantitative visualization of the data. In Figs. 4(a) and 4(b) we plot the results for the input SOPs X (violet) and Y (green), in Figs. 4(c) and 4(d) for the input SOPs 45 (violet) and -45 (green), and in Figs. 4(e) and 4(f) for the input SOPs R (violet) and L (green).

In the Poincaré sphere representations [Figs. 4(a), 4(c), and 4(e)] we see that the output trajectories for any two orthogonal incident SOPs are orthogonal to each other, thus they correspond to orthogonal reflected SOPs. This can be more precisely seen in the azimuth and ellipticity representation, where we see that there is a 90º difference in the azimuth for the two reflected SOPs and the ellipticities are symmetrical with respect to the X-axis in the plot. The orthogonality condition is verified by homogeneous polarization systems [29, 30]. Thus, the LCoS can be considered as a homogeneous system, at least when considering the fully polarized component of the measured Stokes vector. In a homogenous system the two eigenstates are orthogonal to each other, and the diattenuation and retardance vectors are parallel to each other and they are along the direction of the two eigenstates [29]. In the present work, the homogeneity of the LCoS shows that the diattenuation is negligible, certifying the results presented in Fig. 3(b).

A qualitative discussion of Fig. 4 at the low and at the high gray level ranges provides some interesting information about the performance of the LCoS as a retarder. First, if we look at the low gray level range, corresponding to the low voltage region, we see that the results approximately verify that incident SOP X (Y) is reflected as SOP X (Y) [Fig. 4(b)], incident SOP 45 (-45) is reflected as SOP L (R) [Fig. 4(d)], and incident SOP R (L) is reflected as SOP 45 (-45) [Fig. 4(f)]. To analyse specifically the performance of the LCoS we must remove the effect introduced in the results by the inversion of the Y-axis between the forward and backward reference systems. Taking this into account, the results in the forward reference system are rewritten as: incident SOP X (Y) is reflected as SOP X (Y), incident SOP 45 (-45) is reflected as SOP R (L), and incident SOP R (L) is reflected as SOP -45 (45). Therefore, it can be said that for the low gray level range the LCoS behaves as a quarter wave plate, with its slow axis along the vertical of the lab. Second, if we analyse the high gray level range, corresponding to the high voltage region, we obtain that incident SOP X (Y) is reflected as SOP Y (X) [Fig. 4(b)], incident SOP 45 (-45) is reflected as SOP -45 (45) [Fig. 4(d)], and incident SOP R (L) is reflected as SOP R (L) [Fig. 4(f)]. When rewriting these results in the forward reference system we obtain: incident SOP X (Y) is reflected as SOP Y

#86144 - $15.00 USD Received 8 Aug 2007; revised 18 Oct 2007; accepted 18 Oct 2007; published 24 Jan 2008

(X), incident SOP 45 (-45) is reflected as SOP 45 (-45), and incident SOP R (L) is reflected as SOP L (R). From these results we conclude that in the high gray level range the LCoS behaves approximately as a half wave plate, with its neutral lines at 45º from the vertical of the lab.

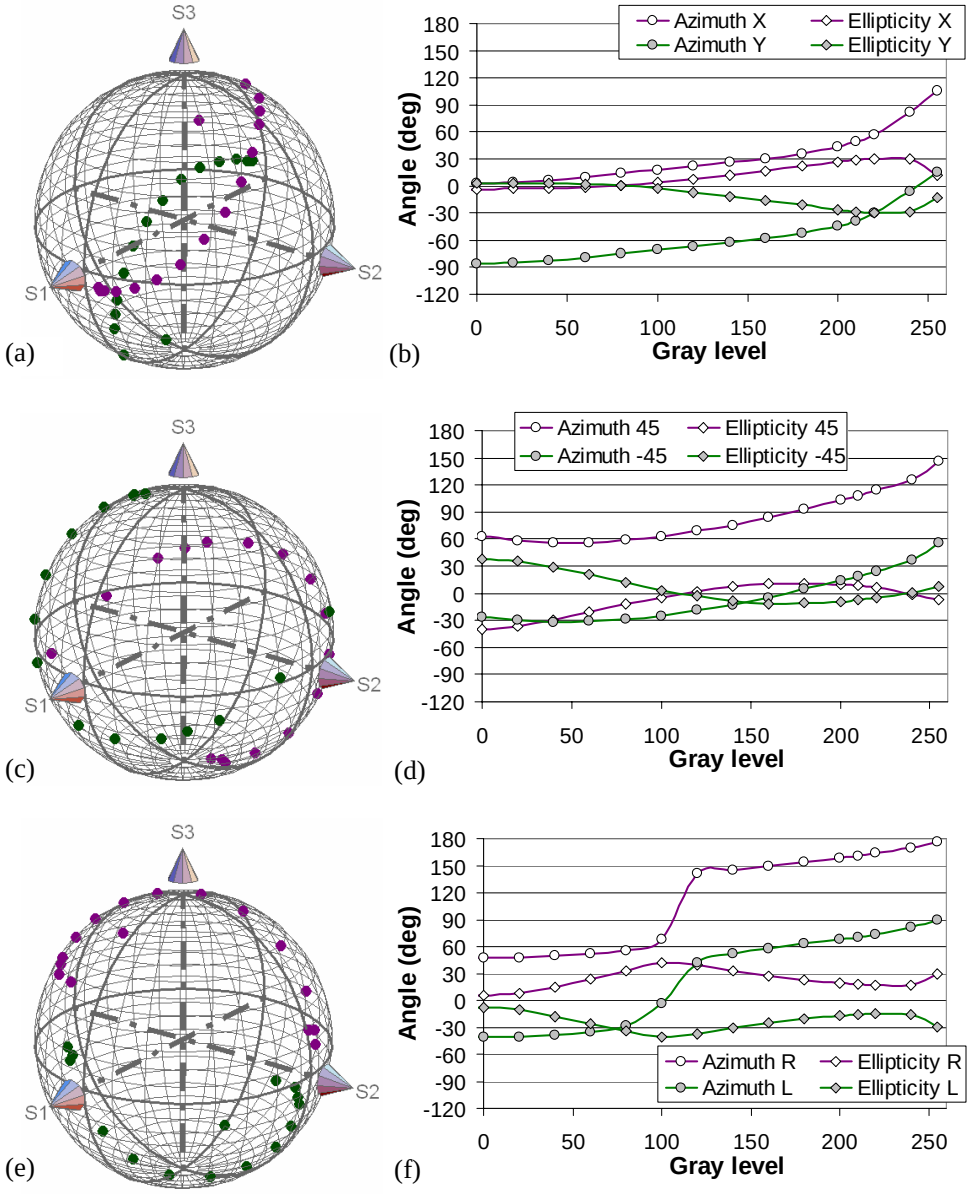

Fig. 4. Normalized Stokes parameters for the full polarized component and for the 6 input SOPs (X, Y, 45, -45, R and L), represented on the Poincaré sphere ((a), (c) and (e)), and azimuth and ellipticity representation as a function of the gray level ((b), (d) and (f)).

From this discussion in the limits of low and high gray levels we see that the LCoS behaves as a linear retarder whose retardance and orientation of its neutral lines vary with the voltage. In the literature [31, 32] it is demonstrated that non-absorbing reciprocal polarization devices behave as linear retarders in reflection. A discussion of the linear retardance exhibited by a LCoS is given by Wolfe and Chipman in Ref. [26], where the measurements are taken at

#86144 - $15.00 USD Received 8 Aug 2007; revised 18 Oct 2007; accepted 18 Oct 2007; published 24 Jan 2008

the gray levels providing the dark and white states when using the LCoS in display applications. Wolfe and Chipman also measured the diattenuation and the depolarization exhibited by a LCoS. They obtained that the diattenuation was negligible and that the depolarization attained values of a 10% when addressing the white state. Our results are very similar to the ones obtained in Ref. [26].

We note that the retardance performance shown by the device at low and at high gray level ranges is consistent with the application as a display for which the LCoS are produced. When used in display systems, the LCoS is typically inserted between a pair of crossed polarizers or used with a polarizing beam splitter, and their axes are along the vertical and horizontal of the lab [9,26]. The LCoS presented in this work provides the dark and the white states needed in display applications respectively at low and at high gray levels when impinging with a linear SOP parallel to the vertical (or horizontal) of the lab.

2.3 Origin for the depolarization: fluctuations of the reflected SOP during the frame period

To obtain further insight into the origin of the depolarization reported in Fig. 2 we have measured the instantaneous optical intensity transmitted by the LCoS sandwiched between two polarizers. For these measurements a digital oscilloscope (Tektronix TDS3012B) has been used. These results were partly presented in [28]. We see in Fig. 5(a) the optical intensity as a function of time with the input and output polarizers at 0º (parallel to the vertical of the lab), and for various constant addressed gray levels. For zero gray level, the intensity is constant in time. However, when the addressed gray level is increased, the optical signal is not constant but oscillates periodically, with a frequency of about 60 Hz (period $\approx$ 17 ms) and a subfrequency of about 120 Hz (period $\approx$ 8 ms). These periodicities are probably related with the frame rate and the field rate of the incoming video signal to the LCoS panel (technical specifications do not offer these details). The oscillations in the optical intensity are very big for gray level 200. The oscillations on the reflected light also depend on the SOP of the incident light. Figure 5(b) shows the results for an addressed gray level 200, for four different orientations of the incident polarizer (0º, 45º, 90º and 135º), and with the analyzer oriented at 0º. We can see that in all cases the optical signal shows great oscillations.

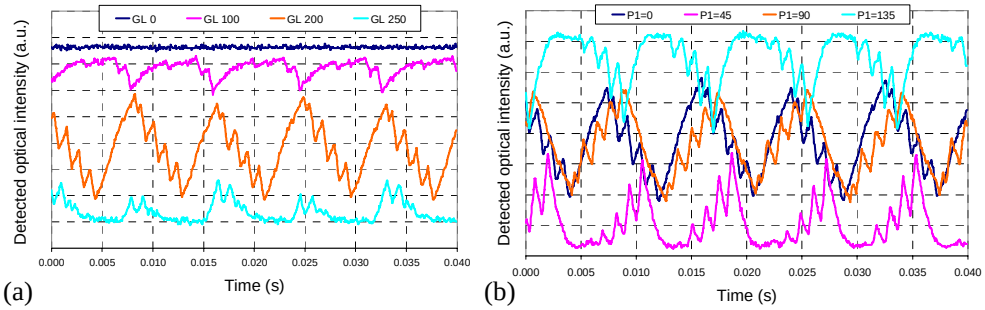

Fig. 5. (a). Optical detected signal with input and output polarizers oriented at 0º, for addressed gray levels (GL) 0, 100, 200 and 250. (b). Detected signal for input polarizer oriented at 0º, 45º, 90º and 135º, with the output polarizer at 0º and for the addressed gray level 200.

The oscillations in the intensity are a consequence of the fluctuation as a function of time of the SOP for the reflected light. Thus, in a frame period the SOP for the reflected light describes a large fluctuation. Temporal averaging of the SOP results in partially polarized light. In Section 2.2 to obtain the Stokes parameters we measured the intensity value shown in the display of the radiometer. This is actually the average intensity value, thus the Stokes vectors measured in Section 2.2 for the 6 different input SOPs correspond to the average reflected SOPs. The SOP time average is usually the interesting magnitude when using the LCoS panel in applications in diffractive optics or optical image processing, where the integration time of the detector is typically much larger than the frame period. We attribute

#86144 - $15.00 USD Received 8 Aug 2007; revised 18 Oct 2007; accepted 18 Oct 2007; published 24 Jan 2008

these oscillations in the reflected SOP to the characteristics of the electrical signal addressing to the display: the voltage across the display is not stable enough during a frame period.

3. Mueller matrix predictive capability

Using the Stokes vectors measured in Section 2 for the 6 input SOPs generated by the PSG we can calculate the 16 elements m_{ij}, where i and j are respectively the row and column indexes, for the Mueller matrix of the LCoS. We have done an extra measurement: the incident intensity onto the LCoS for each of the 6 input SOPs has also been measured to normalize the corresponding Stokes vectors. Since the reflected Stokes vectors vary with the gray level, a different Mueller matrix will be obtained accordingly at each gray level. In Fig. 6 we show the values obtained for the 16 elements of the matrix as a function of the addressed gray level: we plot the values for the elements of the first, second, third and fourth rows respectively in Figs. 6(a), 6(b), 6(c) and 6(d).

Due to the normalization of the measured Stokes vectors by the intensity incident onto the LCoS, the value calculated for the element m_{00} [Fig. 6(a)] is actually the intensity reflectance for the LCoS. This value is less than one due to some light absorption produced in the LCoS but mainly because the measurements for the reflected light are taken at the zero order caused by the pixelation. We see that almost an 80% of the intensity is reflected into the zero order, which is a very high value in accordance with the high fill factor value of 93% reported for the LCoS we are using. The maximum and minimum values for the elements in the matrix are bounded between $\pm m_{00}$. In Fig. 6(a) we see that the values for the elements m_{01}, m_{02} and m_{03} are almost zero. They are in fact equal respectively to the diattenuation coefficients D_X, D_{45} and D_C multiplied by m_{00}. The elements in the first column m_{10}, m_{20} and m_{30}, the polarizance coefficients, show the capability of the device to polarize natural light [22]. We see that in all cases they are practically zero. The submatrix 3x3 obtained taking out the first column and the first row contains the information about retardance and depolarization of the LCoS. We see that the elements in this submatrix present large variations with the gray level, in accordance with the change in the retarder characteristics of the LCoS reported in Section 2.2.

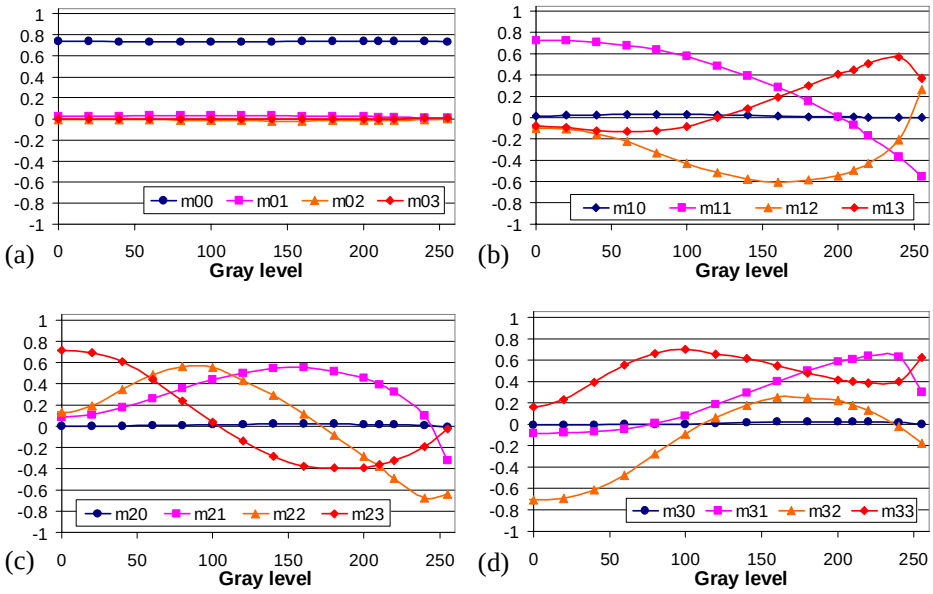

Fig. 6. Values for the elements of the Mueller matrix for the LCoS as a function of the addressed gray level.

#86144 - $15.00 USD Received 8 Aug 2007; revised 18 Oct 2007; accepted 18 Oct 2007; published 24 Jan 2008

We are mainly interested in using the Mueller matrix for the LCoS to calculate the reflected SOP and the intensity transmission of the device for any incident SOP. If the Mueller matrix obtained is able to provide accurate quantitative calculations, we can use it to optimize the orientation of the external polarization elements to produce particular intensity transmission modulations which may be interesting for certain applications.

Next we want to verify the accuracy of the calculations provided by the Mueller matrix. To this goal we have measured the Stokes vector for an arbitrary input SOP. In particular, we have considered linearly polarized light oriented at 30º from the X axis (vertical of the lab). In Fig. 7 we show both the experimental measurements (symbols) and the theoretical values (continuous lines) calculated using for each gray level the experimental Mueller matrix whose coefficients are represented in Fig.6. In Fig. 7(a) we plot DoP and the Stokes parameters (S_0, S_1, S_2 and S_3) for the reflected light. To obtain the Stokes parameters we normalize the reflected intensities by the incident intensity onto the LCoS as explained in the first paragraph in this Section, thus S_0 is actually the intensity reflectance for the LCoS. We see that there is an excellent agreement between experiment and calculations. In Fig. 7(b) we show the representation on the Poincaré sphere for the normalized Stokes vector $(1\ S_{n1}\ S_{n2}\ S_{n3})^{\perp}$ calculated as given in Eq. (6), which represent the fully polarized light component for the reflected SOP. Once again there is an excellent agreement between the experimental values and the data calculated from the Mueller matrix for the LCoS. From the results in Fig. 7 we can say that the Mueller matrix evaluated from the measurements provides accurate calculations for the SOP reflected by the LCoS.

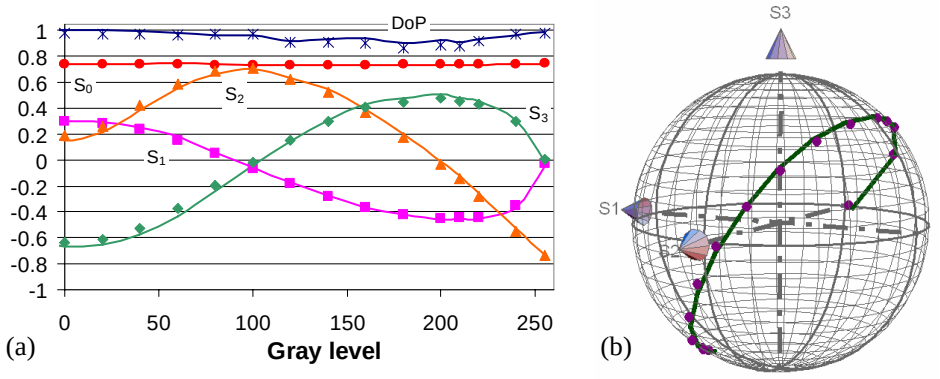

Fig. 7. SOP reflected by the LCoS for a linearly polarized incident SOP with 30º azimuth. (a) Representation of the DoP and the Stokes parameters as a function of the gray level; (b) Representation on the Poincaré sphere for the normalized Stokes vector $(1\ S_{n1}\ S_{n2}\ S_{n3})^{\perp}$. Symbols and continuous lines correspond to experimental and theoretical data respectively.

4. Intensity modulation optimization

The accurate predictive capability of the Mueller matrix for arbitrary configurations of the PSG and the PSD can be used to calculate, by means of some numerical search algorithm, the optimum configuration for the PSG and the PSD providing a specific intensity modulation regime. To increase the degrees of freedom in this optimization procedure we should use a PSG and a PSD capable to cover the whole Poincaré sphere, i.e. they must be composed of a linear polarizer and a quarter wave plate retarder. There are a series of modulation regimes which are usually of interest, such as maximum intensity contrast modulation or constant amplitude modulation, as we shall explain in the following subsections. The modulation regime obtained depends on the figure of merit defined for the numerical search and on the starting values given for the parameters.

In this Section we also show measurements for the phase-shift modulation provided by the LCoS. To this goal we construct a two beams Young's fringes based interferometer in

#86144 - $15.00 USD Received 8 Aug 2007; revised 18 Oct 2007; accepted 18 Oct 2007; published 24 Jan 2008

reflection. This interferometer in its transmissive version has been used to characterize the phase-shift modulation of transmissive LCDs [33]. Here we have adapted it for a reflection geometry. A diffraction grating with a low spatial frequency is introduced before the LCoS so that the +1 and -1 diffracted orders impinge onto two separate halves of the LCoS. The zero diffracted order is blocked. The interference between the two reflected beams is magnified by a microscope objective onto a CCD camera. One half of the LCoS is addressed with a constant gray level whereas in the other half the gray level is varied. From the displacement in the interference pattern with the gray level we can extract the phase-shift value. We note that the visibility of the fringes may reduce drastically if the intensity transmission varies largely with the gray level, as it happens in Section 4.1. However, since phase modulation is measured from fringe displacements, this visibility does not lead to a big increase in the error of the measured phase, except when there is a big difference between the intensity levels. For that reason we select the constant reference gray level value, with a moderate intensity transmission, which allows for a reasonable fringes visibility for most of the gray levels. In our case, we obtained good enough visibility in the complete range owing to the use of a high dynamic range camera. If this type of camera is not available, the diffractive method proposed by Engström et al. [34] could be used, since it permits the determination of the phase modulation even if there are nulls in the amplitude transmission.

4.1 Maximum intensity contrast modulation

Maximum intensity contrast modulation is of interest for the LCoS in display applications. Moreover with a low value for the phase-shift modulation an amplitude-mostly regime can be obtained, which is interesting for diffractive optics, optical signal processing, digital-holography, etc. The experience tells us that usually when a maximum intensity contrast configuration is obtained, either this configuration or its biorthogonal will provide a reasonably low phase-shift modulation depth. By biorthogonal we mean the configuration obtained by orienting both the PSG and the PSD to generate and detect respectively the SOPs which are orthogonal to the initial ones, thus the intensity transmission profile is the same as the initial one (note that just orienting orthogonally the PSG or the PSD would provide the complementary intensity transmission). Since this is a heuristic approach it does not allow to assure that the amplitude-mostly configuration obtained may be the optimum one. To this goal we should be able to calculate the phase-shift modulation values as well. For that purpose the Jones matrix formalism is appropriate since it deals directly with field amplitude values. Work in progress in our research team is addressing this issue.

Table 1. Azimuth and ellipticity angles for the SOPs generated and detected by the PSG and the PSD in the optimum modulation configurations. The orientation of the external polarization elements is also indicated.

Configuration	ψ_1 (º)	χ_1 (º)	φ_1 (º)	η_1 (º)	ψ_2 (º)	χ_2 (º)	φ_2 (º)	η_2 (º)
Fig. 8	102	21	-57	12	163	-11	-28	-17
Fig. 10	102	21	-57	12	73	11	62	-17

The figure of merit to search for optimal configurations is usually a trade-off between different criteria as described by Nicolás, *et al*. [8]. In particular, the figure of merit defined to search for a maximum contrast modulation is a trade-off between the following criteria: minimum value of transmittance as low as possible, maximum value of transmittance as high as possible, and monotonous (and if possible linear) variation of the intensity between these maximum and minimum values. In Fig. 8 we show a maximum intensity contrast configuration obtained applying the optimization procedure. In Table 1, second row, we show the azimuth ψ and the ellipticity χ angles for the incident SOP, (ψ_1,χ_1), generated by the PSG and the reflected SOP, (ψ_2,χ_2), to which the PSD is adapted. There is not a unique combination of the elements in the PSG and PSD to generate and detect these SOPs. In Table

#86144 - $15.00 USD Received 8 Aug 2007; revised 18 Oct 2007; accepted 18 Oct 2007; published 24 Jan 2008

1 we give a possible combination for the angles of the polarizer φ and quarter wave plate η in the PSG, (φ_1,η_1), and in the PSD, (φ_2,η_2). We note that the polarizers and quarter wave plates that we use are the same ones introduced in Section 2.1.

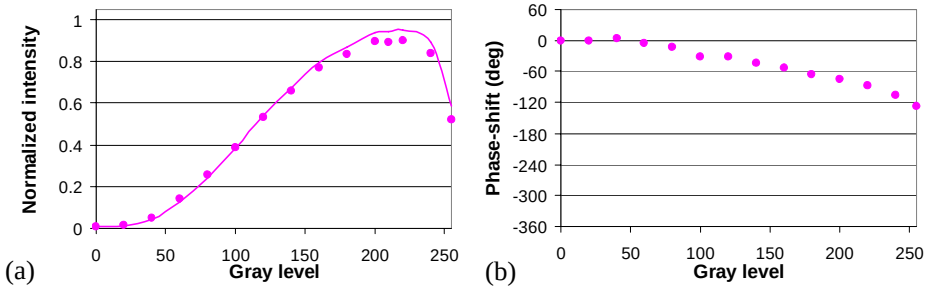

Fig. 8. Maximum intensity contrast. (a). Normalized intensity (theory – line, experiment – symbols. (b). Phase-shift (experimental). Configuration given in Table 1. The low phase-shift depth enables to use this configuration for amplitude-mostly modulation.

In Figs. 8(a) and 8(b) we show respectively the intensity and the phase-shift modulations as a function of the addressed gray level. In the case of the intensity modulation we show both the experimental and the theoretically calculated results. The intensity values are normalized by the total light reflected by the LCoS into the zero order of diffraction produced by the pixelation of the LCoS device. In the case of the phase-shift modulation we plot the experimental measurements. In Fig. 8(a) we see that there is a good intensity contrast achieving both a low intensity value close to zero and a maximum value close to one. The intensity modulation shows a monotonic increase in the gray level range 0-200, which would be the useable range for applications. The agreement between calculations and experiment is very good. From the analysis of the phase-shift modulation [Fig. 8(b)] we see that the phase-shift modulation depth is about 70º in the gray level range 0-200, which is a very low value. Therefore this configuration is not only a maximum intensity contrast modulation but also an amplitude-mostly modulation that is useful for a wider range of applications.

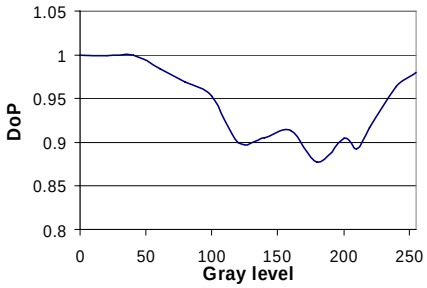

Fig. 9. Theoretical DoP for the SOP reflected by the LCoS. The incident SOP is (ψ_1 = 112º, χ_1 = 21º). This is the incident SOP both in Figs. 8 and 10.

The information provided in Fig. 8 is not complete due to the existence of depolarized light. In this case it becomes important to quantify what is the contribution of the depolarized light to the total value of the normalized intensity. This contribution can be thought as an incoherent background noise which may affect the performance of the LCoS in applications. In the calculations we consider the SOP generated by the PSG for the configuration in Fig. 8, and we obtain the DOP for the SOP reflected by the LCoS as a function of the gray level by using the verified experimental matrices. The results are plotted in Fig. 9. Note that the vertical scale ranges from 0.80 to 1.05. Between gray levels about 120 and 210 there is a 10% of depolarized light. In display applications this depolarized light may act as an incoherent

#86144 - $15.00 USD Received 8 Aug 2007; revised 18 Oct 2007; accepted 18 Oct 2007; published 24 Jan 2008

background noise reducing the contrast of the image. Let us now introduce the PSD corresponding to the configuration in Fig. 8 after the LCoS. Since the PSD contains an analyzer, the component of depolarized light in the total intensity measured after the PSD at a certain gray level is equal to half of the value 1-DoP at this gray level. The other half would be measured with the PSD at the orthogonal orientation. For example, this means that at gray level 200 the depolarized light contributes with a 0.05 to the total value of normalized intensity shown in Fig. 8(a) after the PSD.

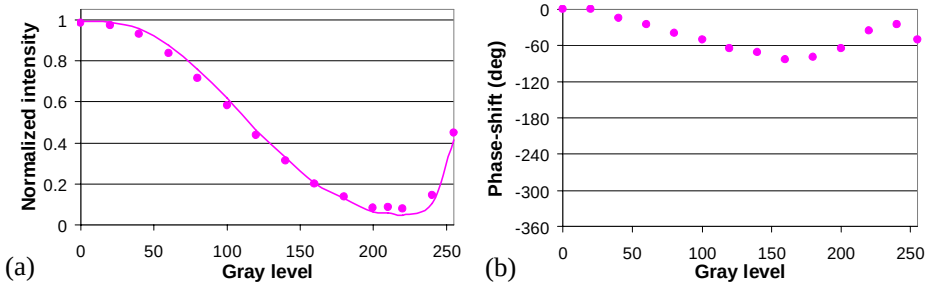

Fig. 10. Results for the PSD orthogonally oriented with respect to the PSD in Fig. 8(a) Normalized intensity (theory – line, experiment – symbols). (b) Phase-shift (experimental). The non-null at gray level 200 is mainly due to depolarized light.

In Figs. 10(a) and 10(b) we show respectively the results when we consider the orthogonal orientation for the PSD with respect to the orientation previously given in Fig. 8. Angles are given in Table 1, third row. In principle, the intensity modulation should be the complementary of the one given in Fig. 8(a). This is actually the case when comparing Figs. 8(a) and 10(a). The minimum value of intensity, at gray level 200, is about 0.05. From the discussion done in Fig. 9, this is actually the value of the depolarized intensity component. Therefore it can be said that depolarization is the responsible for this non-null minimum which avoids this configuration from being a maximum intensity contrast modulation configuration. In Fig. 10(b) we see that the phase-shift modulation depth is very low (about 80º). This could have also been an amplitude-mostly modulation configuration if depolarization was not present.

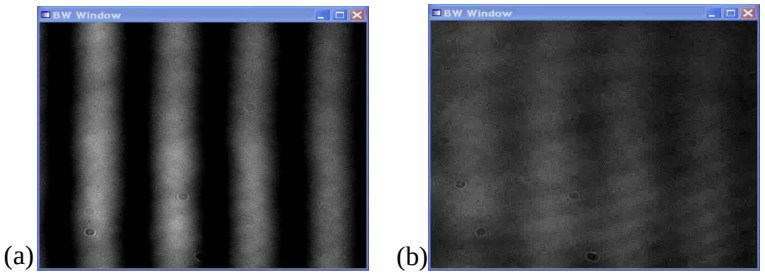

Fig. 11. Video files recorded for the interference pattern for the configuration presented in Fig. 10. The two halves of the LCoS are addressed respectively with gray levels 0 and 20 in (a) (Movie 1: 2.3 MB), and with gray levels 40 and 200 in (b) (Movie 2: 2.5 MB).

In Fig. 11 we show two video files which record the interference pattern when measuring the phase with the Young's fringes based interferometer. To record the videos we have used a CCD camera, model pco.2000 by pco.imaging. This is a high dynamic range camera with 14 bits of digitization. The high dynamic range was necessary to enhance the visibility of the fringes when the transmission of the two halves of the LCoS is very dissimilar. We note that the initial duration of the video recorded is only a few periods of the LCoS signal. We have slowed down the play back of the video to see the evolution of the fringes during the

#86144 - $15.00 USD Received 8 Aug 2007; revised 18 Oct 2007; accepted 18 Oct 2007; published 24 Jan 2008

addressing of the LCoS. The integration time for each frame composing the video is 1 ms, which according to the intensity fluctuations shown in Fig. 5 should allow to appreciate the instantaneous position of the interference pattern in case it fluctuates. Both videos correspond to the configuration of Fig. 10. Figure 11(a) corresponds to the interference fringes when the two halves of the LCoS are addressed respectively with gray levels 0 and 20. We see in the video that the fringes stay very still during the play back. Figure 11(b) corresponds to the interference fringes when the two halves of the LCoS are addressed respectively with gray levels 40 and 200. In this case we note that the fringe pattern oscillates, and the visibility of the fringes goes practically to zero at certain moments during the addressing of the LCoS.

The time evolution of the fringe pattern shown in Fig. 11(b) is actually in accordance with the temporal averaging origin for the depolarized light commented in Section 2.3. As we said the SOP reflected by the LCoS fluctuates during the time of a frame. If depolarization were due to processes as scattering, then simply there would be no observable interference pattern in Fig. 11(b) when addressing gray level 200 to one of the two halves of the LCoS. In principle from the results presented in this work we may expect that the temporal fluctuations will add some unpolarized light to the temporal averaged SOP. The influence of these fluctuations will depend on the magnitude of the depolarization, which attains the highest values in range about gray level 200. In most applications as in display technology, in diffractive optics, etc, the observed magnitudes are time averaged, and this is what we have considered in all measurements of intensity and phase in this paper.

4.2 Constant intensity modulation

Constant intensity modulation combined with a phase-shift modulation depth about 360º is known as phase-only modulation [8]. From the research experience accumulated with transmissive LCDs we know that constant intensity configurations provide a large phase-shift modulation depth, and if not the biorthogonal configuration does.

Table 2. Azimuth and ellipticity angles for the SOPs generated and detected by the PSG and the PSD in the optimum modulation configurations. The orientation of the external polarization elements is also indicated.

Configuration	ψ_1 (º)	χ_1 (º)	φ_1 (º)	η_1 (º)	ψ_2 (º)	χ_2 (º)	φ_2 (º)	η_2 (º)
Fig. 12	71	0	71	---	129	0	129	---
Fig. 13	70	-25	45	-20	108	-31	-41	18

In Figs. 12(a) and 12(b) we plot respectively the intensity and the phase-shift modulations versus the addressed gray level for optimum configuration obtained using only polarizers in the PSG and PSD. The angles for this configuration are given in Table 2, second row. We see in Fig. 12(a) that the intensity is actually not very constant (almost a 40% of fluctuation). Therefore, we can assure that only polarizers are not able to provide constant intensity modulation, as it is also the case with modern transmissive LCDs which are thin devices [7,8]. We see that once again the agreement between calculations and experiment is very good, confirming the predictive capability of the Mueller matrix. The phase-shift, Fig. 12(b), has a modulation depth of about 240º for this configuration.

In Fig. 13 we consider the PSG and PSD composed of a linear polarizer and a quarter waveplate. In Figs. 13(a) and 13(b) we observe respectively the intensity and the phase-shift modulations versus the addressed gray level for the optimum configuration. The angles for this configuration are given in Table 2, third row. We see that the normalized intensity curve [Fig. 13(a)] is very high and the fluctuations are small (about a 10%), thus it is a good constant amplitude configuration. The phase-shift [Figs. 13(b)] in this configuration is close to 300º. It can be considered a phase-mostly modulation. Even though the phase depth is less than 360º, there are some strategies that allow to obtain very efficient results with a phase depth of 300º [35, 36]. Agreement between experiment and calculations of the normalized intensity is very good as in the previous plots.

#86144 - $15.00 USD Received 8 Aug 2007; revised 18 Oct 2007; accepted 18 Oct 2007; published 24 Jan 2008

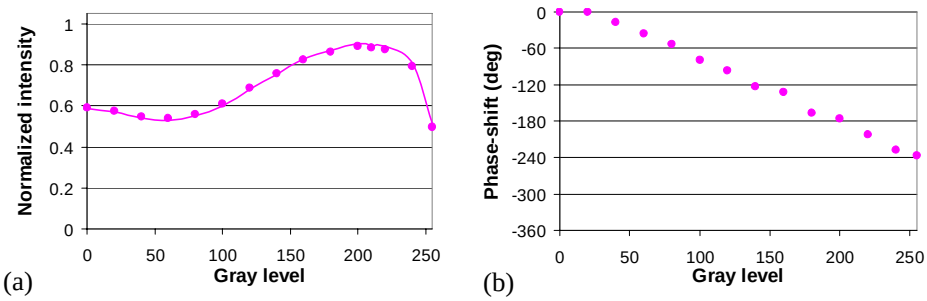

Fig. 12. Modulation in a configuration for constant intensity with only polarizers. (a). Normalized intensity (theory – line, experiment – symbols) and DoP (theory). (b). Phase-shift (experimental). Configuration given in Table 2.

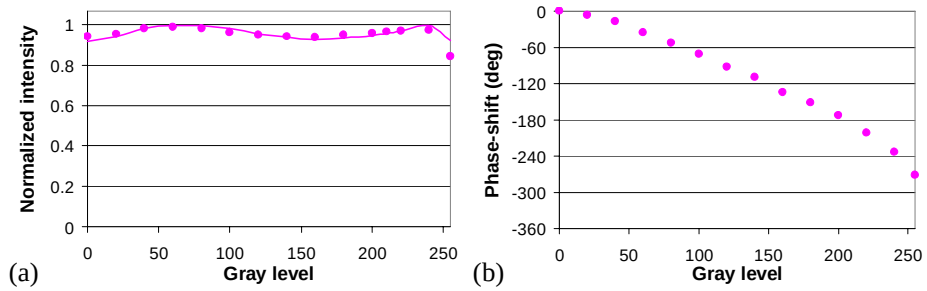

Fig. 13. Modulation in a configuration for constant intensity with elliptically polarized light. (a). Normalized intensity (theory – line, experiment – symbols). (b). Phase-shift (experimental). Configuration given in Table 2. The phase-shift depth close to 300º enables for phase-mostly modulation.

In Fig. 14 we plot the calculated DoP for the SOP reflected by the LCoS as a function of the gray level. Figs. 14(a) and 14(b) are calculated considering the incident SOPs generated by the PSG in the configurations for Figs. 12 and 13 respectively. We note that in both Figs. 14(a) and 14(b) the DoP is very high. Especially in Fig. 14(b) the DoP is almost 100% (values slightly over 100%, are due to the experimental origin for the Mueller matrix for the LCoS used in the calculations).

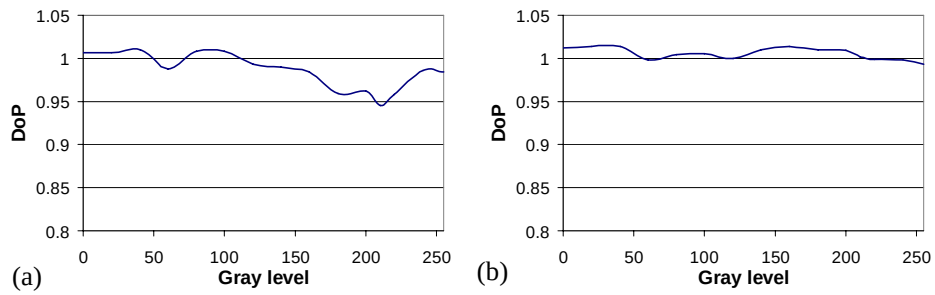

Fig. 14. Theoretical DoP for the SOP reflected by the LCoS. In (a) for the incident SOP used in Fig. 11, and in (b) for the incident SOP used in Fig. 12.

5. Conclusion

In this paper we have characterized the polarimetric properties of a LCoS, including depolarization and diattenuation which are usually not considered when applying the LCoS in diffractive optics. On one hand, we have found that the LCoS generates a certain degree (it

#86144 - $15.00 USD Received 8 Aug 2007; revised 18 Oct 2007; accepted 18 Oct 2007; published 24 Jan 2008

can be larger than a 10%) of depolarized light, which depends on the addressed gray level and on the incident SOP. We relate the main origin of the depolarized light with temporal fluctuations during the time of a frame for the SOP reflected by the LCoS. On the other hand, diattenuation is practically null, thus the LCoS can be basically considered as the combination of a retarder and a depolarizer. Along with the polarimetric characterization we obtain the Mueller matrix of the LCoS as a function of the gray level. We have checked that the Mueller matrix obtained from the measurements is able to predict the reflected SOP. As a consequence the Mueller matrix characterization enables for a numerical search of optimum intensity modulation configurations. In particular we look for maximum contrast modulation or constant intensity modulation. By means of a heuristic approach we have shown that amplitude-mostly modulation and phase-mostly modulation with a large phase-shift depth can be obtained for a wavelength of 633 nm, using elliptically polarized light.

Acknowledgments

We acknowledge financial support from the Spanish Ministerio de Educación y Ciencia (grants FIS2006-13037-C02-01 and FIS2006-13037-C02-02) and from Generalitat de Catalunya (grant ACI2003-42). C. Iemmi gratefully acknowledges the support of the Universidad de Buenos Aires and CONICET (Argentina).

#86144 - $15.00 USD Received 8 Aug 2007; revised 18 Oct 2007; accepted 18 Oct 2007; published 24 Jan 2008